

M₃Ag₁₇(SPh)₁₂ Nanoparticles and Their Structure Prediction

Sameera Wickramasinghe,[†] Aydar Atnagulov,[†] Bokwon Yoon,[§] Robert N. Barnett,[§] Wendell P. Griffith,[†] Uzi Landman,[§] and Terry P. Bigioni^{*,†,‡}

[†]Department of Chemistry and [‡]The School of Solar and Advanced Renewable Energy, University of Toledo, Toledo, Ohio 43606, United States

[§]School of Physics, Georgia Institute of Technology, Atlanta, Georgia 30332-0430, United States

S Supporting Information

ABSTRACT: Although silver nanoparticles are of great fundamental and practical interest, only one structure has been determined thus far: M₄Ag₄₄(SPh)₃₀, where M is a monocation, and SPh is an aromatic thiolate ligand. This is in part due to the fact that no other molecular silver nanoparticles have been synthesized with aromatic thiolate ligands. Here we report the synthesis of M₃Ag₁₇(4-*tert*-butylbenzene-thiol)₁₂, which has good stability and an unusual optical spectrum. We also present a rational strategy for predicting the structure of this molecule. First-principles calculations support the structural model, predict a HOMO–LUMO energy gap of 1.77 eV, and predict a new “monomer mount” capping motif, Ag(SR)₃, for Ag nanoparticles. The calculated optical absorption spectrum is in good correspondence with the measured spectrum. Heteroatom substitution was also used as a structural probe. First-principles calculations based on the structural model predicted a strong preference for a single Au atom substitution in agreement with experiment.

Silver nanoparticles are of significant fundamental and practical interest because of their optical and biological properties. Nevertheless, very little is known about the principles that govern their structures. The precise atomic structures of molecular nanoparticles can be determined by single-crystal X-ray diffraction methods; however, only one silver nanoparticle structure has been determined by single-crystal X-ray diffraction methods thus far: M₄Ag₄₄(SPh)₃₀, where M is a single-charge cationic counterion, and SPh is a thiolate ligand containing a phenyl ring.^{1–4} This provided the first picture of the silver thiolate protective outer layer, which was shown to consist of 3D Ag₂(SPh)₅ mounts.¹ These mounts are very different from the 1D staple motif in the case of thiolate-ligated gold nanoparticles.^{5–8} It remains to be seen, however, whether the Ag₂(SPh)₅ mounts are common to a variety of thiolated silver nanoparticles or whether they are unique for protecting the 32 Ag atom excavated decahedral core of M₄Ag₄₄(SPh)₃₀. Such information is critically important for understanding the principles behind silver nanoparticle structures and developing a general structural model for thiolated silver nanoparticles as well as self-assembled monolayers on silver surfaces.

A large number of phenyl-ring-containing ligands have been used to prepare M₄Ag₄₄(SPh)₃₀ nanoparticles.³ Interestingly,

preparations of M₄Ag₄₄(SPh)₃₀ nanoparticles have yet to yield other species; all appear to be single-sized products. It is somewhat of a challenge, then, to produce other species that may be crystallized for comparison in structural studies because phenyl-ring-containing ligands are important for crystallization. To this end, we have used a bulky phenyl-ring-containing ligand, 4-*tert*-butylbenzenethiol (TBBT), to change the interligand interactions and thereby induce the formation of a new silver nanoparticle species. Herein we report the synthesis of M₃Ag₁₇(TBBT)₁₂ nanoparticles, their salient physical properties, and a compelling structural model that introduces a new silver thiolate mount motif.

The M₃Ag₁₇(TBBT)₁₂ nanoparticles were synthesized by a method that was similar to a previous report.³ Silver nitrate (0.714 mmol) was dissolved along with TBBT (0.500 mmol) in 7.20 mL of dimethylformamide (DMF) and then stirred for 15 min. This mixture formed a yellow precipitate, which was the silver thiolate precursor. The precursor was reduced with 28.6 mL of a DMF solution of NaBH₄ (2.86 mmol), which was added dropwise. The cloudy yellow mixture changed to form a clear orange solution that darkened over time as it was stirred for 3 h. The color at this stage was dominated by larger plasmonic species, as verified by absorption spectroscopy;⁴ however, a new peak was also present near 443 nm (Figure S3). Next, 4.20 mL of deionized water was added to increase the reduction potential of the NaBH₄. This also sped up the reaction; therefore, the solution was left to incubate for 16 h at –18 °C. Over this time, a dark precipitate formed, and the optical density of the solution decreased. Presumably, the precipitate was formed from the larger silver nanoparticles that were observed before the addition of water. The final solution was clear and yellow in color.

The product of this reaction was analyzed by electrospray-ionization mass spectrometry (ESI-MS), which revealed the presence of a new silver nanoparticle: Ag₁₇(TBBT)₁₂^{3–} (Figure 1). Such a species has not been observed in any other preparation of silver molecular nanoparticles with either aromatic^{1–3,9} or aliphatic^{10–12} thiolate ligands. Only a small amount of one fragment species was observed, namely, Ag₁₇(TBBT)₁₁^{2–}, indicating that Ag₁₇(TBBT)₁₂^{3–} was quite stable for the conditions of the measurement (Figure S1). No charge state distribution was observed because the TBBT ligand is aprotic. Other species observed included adducts of

Received: May 31, 2015

Published: August 24, 2015



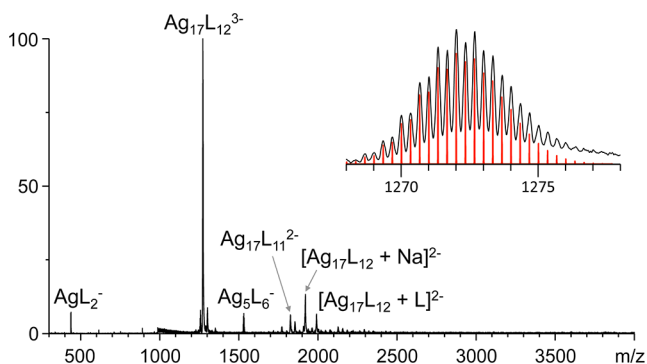


Figure 1. Electrospray-ionization mass spectrum of Ag:TBBT nanoparticles, showing $\text{Ag}_{17}(\text{TBBT})_{12}^{3-}$ along with other species. Inset: experimental (black) and simulated (red) isotopic patterns for $\text{Ag}_{17}\text{L}_{12}^{3-}$, where L = TBBT, with a shift of 0.08 m/z to correct for a 63 ppm mass difference due to external calibration.

the parent compound along with $\text{Ag}(\text{TBBT})_2^-$ and $\text{Ag}_5(\text{TBBT})_6^-$, which may have been solution-phase decomposition products.¹³ No $\text{Ag}_{44}(\text{TBBT})_{30}^{4-}$ was observed, consistent with optical measurements.

The dark-yellow supernatant had a single strong absorption peak located at 424 nm that dominated the optical absorption spectrum, unlike any previously observed, with two small features on either side and a slowly decaying low-energy tail (Figures 3 and S4). The prominent peak at 424 nm is much narrower (0.18 eV fwhm) and located to the red of a typical plasmon peak characteristic of a spherical silver nanoparticle.^{14,15} None of the spectral features characteristic of $\text{Na}_4\text{Ag}_{44}(\text{TBBT})_{30}$ were observed in the spectrum, which is consistent with the ESI-MS results.

X-ray data are not always available for structure determination; therefore, structure prediction methods are needed. The prediction of structures of gold and silver molecular nanoparticles presents one of the foremost challenges in molecular nanoparticle science, however, and has yet to yield a definite successful example. The small size of $\text{M}_3\text{Ag}_{17}(\text{TBBT})_{12}$ as well as past lessons learned provide an opportunity to begin the formulation of guiding principles for structure prediction and to attempt the prediction of a verifiable structure of this molecular nanoparticle.

First, it is well-known that very small metal particles tend to assume low-energy icosahedral structures.^{16,17} Gold and silver molecular nanoparticles share this tendency because the cores of many known structures contain icosahedra, with few exceptions; therefore, it is reasonable to begin a structural model with an icosahedral core. Second, it is also well-known that the presence of a central atom in the icosahedral core affects primarily the superatomic S orbitals because of their nonzero amplitude at the origin, i.e., the center of the particle.^{18–20} For example, an 18-electron spherical core will have 1S^2 , 1P^6 , and 1D^{10} occupied orbitals and a 2S orbital as the lowest unoccupied molecular orbital (LUMO);²¹ therefore, an empty 12-atom icosahedron would be favored because it would raise the energy of the 2S LUMO and thereby increase the energy gap. This is the case for $\text{M}_4\text{Ag}_{44}(\text{SPh})_{30}$.^{1,2}

Formal counting²² for $\text{M}_3\text{Ag}_{17}(\text{TBBT})_{12}$ nanoparticles gives eight delocalized electrons, which are expected to fill the 1S^2 and 1P^6 orbitals²¹ so that the highest occupied molecular orbital (HOMO) is 1P and the LUMO is 1D. This is indeed found from our density functional theory (DFT) electronic

structure calculations (see below); therefore, there is no electronic advantage to an empty 12-atom icosahedral core. This is generally the case for an eight-electron core, such as $\text{MAu}_{25}(\text{SR})_{18}$.^{6,7} In contrast, there is an energetic advantage to a 13-atom (atom-centered) icosahedral core because of the coordination of the central atom. We therefore predict $\text{Na}_3\text{Ag}_{17}(\text{TBBT})_{12}$ to have a 13-atom icosahedral core, as shown in Figure 2a.

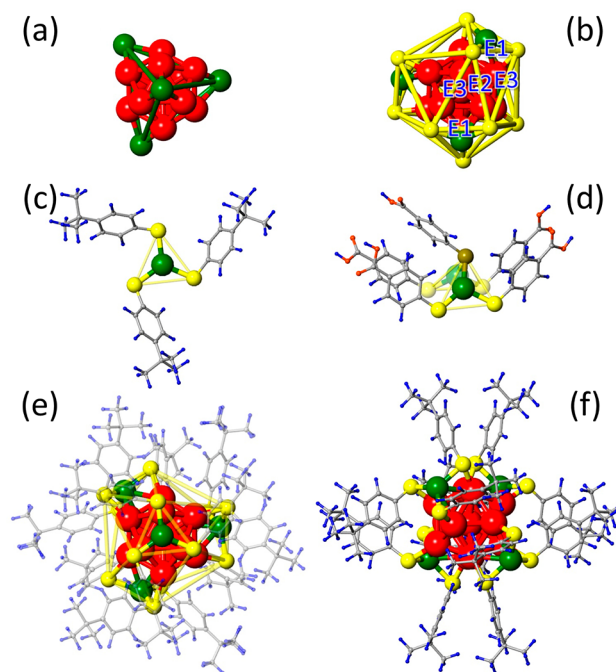


Figure 2. Proposed structure for $\text{M}_3\text{Ag}_{17}(\text{TBBT})_{12}$ nanoparticles, constructed and relaxed with DFT calculations. (a) The structure consists of an icosahedral Ag_{13} core (red) capped with four tetrahedrally located Ag atoms (green). (b) Twelve sulfur atoms (yellow) surround the silver core, with three S atoms forming an equilateral triangle around each tetrahedrally located Ag atom, to form a distorted icosahedron (yellow lines); E1, E2, and E3 are different edge lengths. (c) Isolated view of a $\text{Ag}(\text{TBBT})_3$ monomer unit structure; the S atoms form an equilateral triangle (yellow lines). Carbon atoms are gray, and hydrogen atoms are blue. (d) Isolated view of the $\text{Ag}_2(\text{pMBA})_5$ dimer mount structure found on the $\text{Na}_4\text{Ag}_{44}(\text{pMBA})_{30}$ molecule; for comparison see ref 1. The S atoms form nearly equilateral triangles (yellow lines); oxygen atoms are in orange. (e) View of the $\text{M}_3\text{Ag}_{17}(\text{TBBT})_{12}$ structure down the threefold axis, showing slight rotation between the mount and the underlying icosahedral core. (f) View showing face-to-face interactions of the phenyl rings of ligands on neighboring mounts, leading to an overall octahedral arrangement of ligand bundles.

Next, we consider the ligand shell. In the case of gold molecular nanoparticles, the capping motif has consistently been shown to be monomer and dimer staples.^{5–8} These can be thought of as fragments of the linear gold thiolate polymer, $p\text{-(AuSR)}_n$. For silver, the capping motif for $\text{M}_4\text{Ag}_{44}(\text{SPh})_{30}$ nanoparticles was carefully analyzed and has been shown to be the aforementioned $\text{Ag}_2(\text{SPh})_5$ mount.¹ This is a 3D structure and is therefore distinct from the linear gold thiolate polymer. The fact that $\text{Ag}_2(\text{SPh})_5$ mounts were observed instead of staples can be understood on the basis of the topological difference between the bonding of gold and silver in metal thiolates, which are two- and three-coordinate, respectively.²³

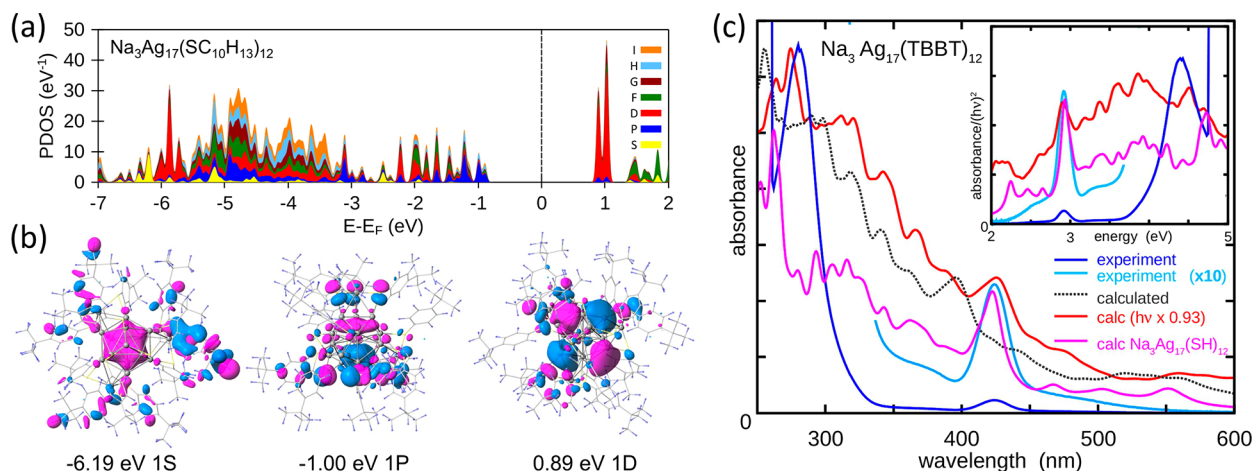


Figure 3. Electronic properties. (a) Projected DOS calculated for the relaxed $\text{Na}_3\text{Ag}_{17}(\text{TBBT})_{12}$ structure. The color-coded angular momenta are given on the right. (b) Representative wave function portraits corresponding to the indicated energies are given at the bottom. (Blue and purple signify different signs.) The nodal structures for the delocalized orbitals with eigenenergies -6.19 , -1.00 , and 0.89 eV correspond to 1S, 1P (HOMO) and 1D (LUMO) superatom states. The Fermi energy, at $E_F = 0.0$ eV, is indicated by the dashed line. (c) Measured (dark and light-blue lines) and TD-DFT-calculated (red and dotted black lines) optical absorption spectra of $\text{Na}_3\text{Ag}_{17}(\text{TBBT})_{12}$ nanoparticles and calculated spectrum for $\text{Na}_3\text{Ag}_{17}(\text{SH})_{12}$ (pink) plotted vs wavelength and energy (inset). The dotted black line is the as-calculated spectrum, and the red line is obtained by scaling the as-calculated spectrum.

Using this example, the 4 Ag atoms and 12 ligands that remain after accounting for the Ag_{13} core can be grouped into 4 trigonal quasi-planar $\text{Ag}(\text{SPh})_3$ mounts, as shown in Figure 2c. These can be thought of as fragments of the 2D silver-thiolate polymer.²⁴ In fact, the $\text{Ag}(\text{SPh})_3$ mount could be considered to be the primitive capping unit for silver thiolate ligands because $\text{Ag}_2(\text{SPh})_5$ mounts can be constructed by fusing two $\text{Ag}(\text{SPh})_3$ mounts. (See Figure 2d, where two of the newly proposed $\text{Ag}(\text{SPh})_3$ mounts are joined at the apex S atom with the elimination of a single thiolate.) In analogy to monomer and dimer staples for gold thiolate ligands,^{5–8} the $\text{Ag}(\text{SPh})_3$ and $\text{Ag}_2(\text{SPh})_5$ capping units can be thought of as monomer and dimer mounts.

Because icosahedra contain the tetrahedral symmetry group, it is possible to arrange the four trigonal planar $\text{Ag}(\text{SPh})_3$ mounts symmetrically around the Ag_{13} core, as shown in Figure 2e. Structural optimization of the molecule with the use of first-principles relaxation revealed that interactions between ligands on neighboring mounts lead to ligand pair bundling,²⁵ resulting in a ligand shell structure with an overall octahedral arrangement (Figure 2f). Here, the ligands tilt in order to maximize the interligand interaction, thereby facilitating face-to-face interactions between the rings with minimal interference from the *tert*-butyl groups. This ligand pair bundling and the symmetry that it confers on the ligand shell are likely to assist in the crystallization of these molecular nanoparticles and influence the properties of the resulting superlattice.²⁶

The stability of the proposed structure is strongly supported by the results of our DFT calculations (Supporting Information), which reveal a density of states (DOS) with a large HOMO–LUMO energy gap $E_{\text{gap}} = 1.77$ eV (Figure 3a). Such a large predicted gap is consistent with experimental ESI-MS measurements of marked gas-phase stability (Supporting Information). Furthermore, the projection of the wave functions onto their angular momenta components shows the expected superatom shell structure with occupied 1S^2 and HOMO 1P^6 delocalized orbitals and superatom LUMO 1D orbitals. (See wave function portraits in Figure 3b.)

The calculated time-dependent DFT (TD-DFT) optical absorption spectrum (Supporting Information, section S5) is in good correspondence with the measured one, lending further support to the proposed structural model (Figure 3c). The experimental spectrum was measured in DMF, and the theoretical spectrum was calculated in vacuum. Thus, redshift-scaling was applied to the calculated spectrum to simulate a solvatochromic effect so that the main prominent absorption feature near 400 nm matched (Figures 3c and S6). The observed absorption features for $\text{M}_3\text{Ag}_{17}(\text{TBBT})_{12}$ are at (A) 424 nm (2.92 eV) and (B) at 280 nm (4.43 eV). For $\text{M}_3\text{AuAg}_{16}(\text{TBBT})_{12}$ these features are found at (A') 408 nm (3.04 eV) and (B') 281 nm (4.41 eV) (Figure S6).

In the calculated spectrum for $\text{Na}_3\text{Ag}_{17}(\text{TBBT})_{12}$, the main absorption features are at (A) 396 nm (3.13 eV) and (B) at 256 nm (4.85 eV). Feature A at 396 nm (3.13 eV) originates from (i) occupied states at -2.33 eV lying mostly on the phenyl rings, excited to the LUMO (0.89 eV) and LUMO+1 1D superatom states on the metal core, (ii) occupied states on the sulfur and silver (d states) atoms at -1.97 eV, excited to the 1D superatom states, and (iii) the HOMO superatom 1P state excited to unoccupied states at 2.30 eV on the phenyl ring. For feature B, the calculated peak occurs at 256 nm (4.85 eV), and it originates from (i) phenyl π -states at -2.31 eV, excited to π^* states at 2.51 eV hybridized in part with sulfur states, (ii) d-band Ag and sulfur states at -1.97 eV, excited to phenyl and ligand states at 2.81 eV, and (iii) d-band metal states at -3.7 to -3.9 eV, excited to the unoccupied 1D superatom states near 1.01 eV.

The calculated spectrum for $\text{Na}_3\text{Ag}_{17}(\text{SH})_{12}$ (pink in Figure 3c) illustrates enhancement of the main observed spectral features (peaks A and B) by suppressing contributions from transitions involving ligand states. (See the region between 300 to 400 nm.) The latter are expected to be more susceptible to smearing of spectral features because of solvent effects and fluctuations, as evidenced in the solution-phase spectra.

Heteroatom substitution was used as a structural probe of $\text{M}_3\text{Ag}_{17}(\text{TBBT})_{12}$. DFT calculations using our model structure predicted a strong preference for a single Au atom substitution

(0.89 eV stabilization for an optimal geometry with the central Ag atom substituted), accompanied by a gap of $E_{\text{gap}} = 1.81$ eV, compared to 1.83 eV for a two-atom Au substitution and 1.77 eV for the all-Ag structure which was confirmed by experiment. Namely, when a stoichiometric 1:16 Au/Ag input ratio was used, $\text{M}_3\text{AuAg}_{16}(\text{TBBT})_{12}$ was produced with only a minor component of $\text{M}_3\text{Au}_2\text{Ag}_{15}(\text{TBBT})_{12}$; no $\text{M}_3\text{Ag}_{17}(\text{TBBT})_{12}$ was detected. When a fivefold excess of Au was used (5:16 Au/Ag input ratio), the results of the synthesis were unchanged. (See Supporting Information for details.)

We have presented experimental results showing the existence of $\text{M}_3\text{Ag}_{17}(\text{TBBT})_{12}$. The structure of this new molecular silver nanoparticle is predicted to consist of a Ag_{13} icosahedral core that is surrounded by a tetrahedral arrangement of newly found $\text{Ag}(\text{SPh})_3$ planar mounts. A rational strategy for predicting the structure of this molecule and calculations that support the structural model were discussed. This work presents an important step toward the goal of developing accurate predictive structural models in order to relieve the crystallization bottleneck that currently limits the structural data available for silver and other metals.

■ ASSOCIATED CONTENT

● Supporting Information

The Supporting Information is available free of charge on the ACS Publications website at DOI: 10.1021/jacs.5b05422.

Additional details regarding the syntheses, ESI-MS measurements, and theoretical analyses are supplied as Supporting Information. (PDF)

■ AUTHOR INFORMATION

Corresponding Author

*E-mail: Terry.Bigioni@utoledo.edu.

Notes

The authors declare no competing financial interest.

■ ACKNOWLEDGMENTS

We thank Dr. Constantine Yannouleas for helpful discussions. Work at the University of Toledo was supported by NSF grant CBET-0955148 and the School of Solar and Advanced Renewable Energy. B.Y. was supported by grant FA9550-14-1-0005 from the Air Force Office of Scientific Research, and R.N.B. and U.L. by the Office of Basic Energy Sciences of the US Department of Energy under contract no. FG05-86ER45234. Calculations were carried out at the Georgia Tech Center for Computational Materials Science.

■ REFERENCES

- (1) Desireddy, A.; Conn, B. E.; Guo, J.; Yoon, B.; Barnett, R. N.; Monahan, B. M.; Kirschbaum, K.; Griffith, W. P.; Whetten, R. L.; Landman, U.; Bigioni, T. P. *Nature* **2013**, *501*, 399–402.
- (2) Yang, H.; Wang, Y.; Huang, H.; Gell, L.; Lehtovaara, L.; Malola, S.; Häkkinen, H.; Zheng, N. *Nat. Commun.* **2013**, *4*, 2422.
- (3) Bakr, O. M.; Amendola, V.; Aikens, C. M.; Wenseleers, W.; Li, R.; Dal Negro, L.; Schatz, G. C.; Stellacci, F. *Angew. Chem., Int. Ed.* **2009**, *48*, 5921–5926.
- (4) Conn, B. E.; Desireddy, A.; Atmagulov, A.; Wickramasinghe, S.; Bhattarai, B.; Yoon, B.; Barnett, R. N.; Abdollahian, Y.; Kim, Y. W.; Griffith, W. P.; Oliver, S. R. J.; Landman, U.; Bigioni, T. P. *J. Phys. Chem. C* **2015**, *119*, 11238–11249.
- (5) Jadzinsky, P. D.; Calero, G.; Ackerson, C. J.; Bushnell, D. A.; Kornberg, R. D. *Science* **2007**, *318*, 430–433.

- (6) Heaven, M. W.; Dass, A.; White, P. S.; Holt, K. M.; Murray, R. W. *J. Am. Chem. Soc.* **2008**, *130*, 3754–3755.
- (7) Zhu, M.; Aikens, C. M.; Hollander, F. J.; Schatz, G. C.; Jin, R. *J. Am. Chem. Soc.* **2008**, *130*, 5883–5885.
- (8) Qian, H.; Eckenhoff, W. T.; Zhu, Y.; Pintauer, T.; Jin, R. *J. Am. Chem. Soc.* **2010**, *132*, 8280–8281.
- (9) Chakraborty, I.; Kurashige, W.; Kanehira, K.; Gell, L.; Häkkinen, H.; Negishi, Y.; Pradeep, T. *J. Phys. Chem. Lett.* **2013**, *4*, 3351–3355.
- (10) Cathcart, N.; Kitaev, V. *J. Phys. Chem. C* **2010**, *114*, 16010–16017.
- (11) Kumar, S.; Bolan, M. D.; Bigioni, T. P. *J. Am. Chem. Soc.* **2010**, *132*, 13141–13143.
- (12) Chakraborty, I.; Govindarajan, A.; Erusappan, J.; Ghosh, A.; Pradeep, T.; Yoon, B.; Whetten, R. L.; Landman, U. *Nano Lett.* **2012**, *12*, 5861–5866.
- (13) Desireddy, A.; Kumar, S.; Guo, J.; Bolan, M. D.; Griffith, W. P.; Bigioni, T. P. *Nanoscale* **2013**, *5*, 2036–2044.
- (14) Mulvaney, P. *Langmuir* **1996**, *12*, 788–800.
- (15) Peng, S.; McMahon, J. M.; Schatz, G. C.; Gray, S. K.; Sun, Y. *Proc. Natl. Acad. Sci. U. S. A.* **2010**, *107*, 14530–14534.
- (16) Frank, F. C. *Proc. R. Soc. London, Ser. A* **1952**, *215*, 43–46.
- (17) Kelton, K. F.; Lee, G. W.; Gangopadhyay, A. K.; Hyers, R. W.; Rathz, T. J.; Rogers, J. R.; Robinson, M. B.; Robinson, D. S. *Phys. Rev. Lett.* **2003**, *90*, 195504.
- (18) Zhang, S. B.; Cohen, M. L.; Chou, M. Y. *Phys. Rev. B: Condens. Matter Mater. Phys.* **1987**, *36*, 3455–3458.
- (19) Baladron, C.; Alonso, J. A. *Phys. B* **1988**, *154*, 73–81.
- (20) Yannouleas, C.; Jena, P.; Khanna, S. N. *Phys. Rev. B: Condens. Matter Mater. Phys.* **1992**, *46*, 9751–9760.
- (21) Knight, W. D.; Clemenger, K.; de Heer, W. A.; Saunders, W. A.; Chou, M. Y.; Cohen, M. L. *Phys. Rev. Lett.* **1984**, *52*, 2141–2143.
- (22) Walter, M.; Akola, J.; Lopez-Acevedo, O.; Jadzinsky, P. D.; Calero, G.; Ackerson, C. J.; Whetten, R. L.; Gronbeck, H.; Häkkinen, H. *Proc. Natl. Acad. Sci. U. S. A.* **2008**, *105*, 9157–9162.
- (23) Dance, I. G. *Polyhedron* **1986**, *5*, 1037–1104.
- (24) Dance, I. G.; Fisher, K. J.; Banda, R. M. H.; Scudder, M. L. *Inorg. Chem.* **1991**, *30*, 183–187.
- (25) Luedtke, W. D.; Landman, U. *J. Phys. Chem.* **1996**, *100*, 13323–13329.
- (26) Yoon, B.; Luedtke, W. D.; Barnett, R. N.; Gao, J.; Desireddy, A.; Conn, B. E.; Bigioni, T. P.; Landman, U. *Nat. Mater.* **2014**, *13*, 807–811.
- (27) AbdulHalim, L. G.; Bootharaju, M. S.; Tang, Q.; Del Gobbo, S.; AbdulHalim, R. G.; Eddaoudi, M.; Jiang, D.-e.; Bakr, O. M. *J. Am. Chem. Soc.* **2015**, DOI: 10.1021/jacs.5b04547.

■ NOTE ADDED IN PROOF

The structure of a 29-atom silver nanoparticle, which shares many features with our work, was recently brought to our attention.²⁷